1521-0111/12/8102-220–227$25.00
MOLECULAR PHARMACOLOGY
Vol. 81, No. 2
74179/3743188

Mol Pharmacol 81:220–227, 2012

Characterization of Multidrug Resistance 1a/P-Glycoprotein Knockout Rats Generated by Zinc Finger Nucleases[S]

Xiaoyan Chu, Zuo Zhang, Jocelyn Yabut, Sarah Horwitz, John Levorse, Xiang-qing Li, Lei Zhu, Harmony Lederman, Rachel Ortiga, John Strauss, Xiaofang Li, Karen A. Owens, Jasminka Dragovic, Thomas Vogt, Raymond Evers, and Myung K. Shin

Pharmacokinetics, Pharmacodynamics and Drug Metabolism (X.C., J.Y., Xiao. Li, K.A.O., J.D., R.E.), Genetically Engineered Model (Z.Z., S.H., J.L., Xian. Li, L.Z., T.V., M.K.S.), Laboratory Animal Resources (H.L.), and Rahway Central Pharmacology (R.O., J.S.), Merck & Co. & Inc., Rahway, New Jersey

Received June 22, 2011; accepted November 2, 2011

ABSTRACT

The development of zinc finger nuclease (ZFN) technology has enabled the genetic engineering of the rat genome. The ability to manipulate the rat genome has great promise to augment the utility of rats for biological and pharmacological studies. A Wistar Hannover rat model lacking the multidrug resistance protein Mdr1a P-glycoprotein (P-gp) was generated using a rat Mdr1a-specific ZFN. Mdr1a was completely absent in tissues, including brain and small intestine, of the knockout rat. Pharmacokinetic studies with the Mdr1a P-gp substrates loperamide, indinavir, and talinolol indicated that Mdr1a was functionally inactive in the blood-brain barrier and intestine in *Mdr1a*(−/−) rats. To identify possible compensatory mechanisms in *Mdr1a*(−/−) rats, the expression levels of drug-metabolizing enzyme and transporter-related genes were compared in brain, liver, kidney, and intestine of male and female *Mdr1a*(−/−) and control rats. In general, alterations in gene expression of these genes in *Mdr1a*(−/−) rats seemed to be modest, with more changes in female than in male rats. Taken together, our studies demonstrate that the ZFN-generated *Mdr1a*(−/−) rat will be a valuable tool for central nervous system drug target validation and determining the role of P-gp in drug absorption and disposition.

Introduction

Gene targeting technology using embryonic stem cells to modify specific alleles in mice has been an invaluable tool to increase the understanding of gene function and disease processes (Capecchi, 2005). However, its ability to specifically target and manipulate the genome of other species has been limited. Notwithstanding, several recent breakthroughs in manipulating the rat genome hold great promise in generating better animal models to study human disease (Hamra, 2010; Tong et al., 2010). The ability to generate genetically altered rat models would be particularly valuable in drug discovery because rats are frequently used as pharmacology models for pharmacokinetic and toxicity studies (Aitman et al., 2008).

One of these promising methods for generating genetically engineered rat models is zinc finger nuclease (ZFN) technology. The ZFN is created by linking zinc finger DNA binding domains (Klug, 2010) to a FokI nuclease domain. The engineered chimeric protein introduces a DNA double-strand break at a predesigned genomic locus (Urnov et al., 2010), which is then repaired by the error-prone nonhomologous end-joining (NHEJ) pathway or the accurate homologous recombination (HR) pathway. The former mechanism results in small deletions or insertions near the repaired region, frequently leading to frameshifts and the creation of a targeted knockout (KO) allele (Urnov et al., 2010). ZFN technology has been successfully used to generate targeted KO rats (Geurts et al., 2009) in a shorter time frame than embryonic stem cell-based gene targeting (Le Provost et al., 2010) and has been applied in other species (Geurts and Moreno, 2010; Urnov et al., 2010).

P-glycoprotein (P-gp, ABCB1) is localized in the plasma membrane of cells where it mediates the ATP-dependent export of drugs (Schinkel and Jonker, 2003; Eyal et al., 2009; Giacomini et al., 2010; Lee et al., 2010). Human MDR1 was first discovered by its overexpression in multidrug-resistant tumor cell lines (Juliano and Ling, 1976), but it is also ex-

X.C. and Z.Z. contributed equally to this work.

Article, publication date, and citation information can be found at http://molpharm.aspetjournals.org.
http://dx.doi.org/10.1124/mol.111.074179.

[S] The online version of this article (available at http://molpharm.aspetjournals.org) contains supplemental material.

ABBREVIATIONS: ZFN, zinc finger nuclease; NHEJ, nonhomologous end-joining; HR, homologous recombination; KO, knockout; P-gp, P-glycoprotein; MDR/Mdr. multidrug resistance; CNS, central nervous system; PCR, polymerase chain reaction; LC, liquid chromatography; MS/MS, tandem mass spectrometry; RT, reverse transcription; q, quantitative; OATP, organic anion-transporting polypeptide; AUC, area under the curve.

pressed in various tissues such as in the luminal membrane of the small intestine, the blood-brain barrier, the apical membrane of hepatocytes, and kidney proximal tubule epithelia (Raub, 2006; Kimura et al., 2007; Miller et al., 2008; Zhou, 2008). In the mouse and rat genome, there are two paralogous genes encoding P-gp: *Mdr1a* and *Mdr1b*, the amino acid sequences of which are 83% identical (Devault and Gros, 1990). On the basis of RNA analysis, mouse Mdr1a is predominantly expressed in intestine, brain, and testis, whereas the expression of Mdr1b is most prominent in the adrenal gland, ovaries, placenta, and kidneys. Both Mdr1a and Mdr1b are also expressed in liver and heart (Schinkel et al., 1994; Chen et al., 2003). P-gp has broad substrate specificity; most of these substrates are neutral and amphipathic positively charged compounds, including many commonly prescribed drugs from various chemical and pharmacological classes (Mahar Doan et al., 2002; Zhou, 2008; Lee et al., 2010).

Mdr1a(−/−) or *Mdr1a/1b*(−/−) mice and Mdr1a-deficient CF-1 mice have been widely used to assess the role of P-gp in vivo (Schinkel et al., 1995, 1996; Schinkel, 1998; Chen et al., 2003). For instance, in vivo studies in *Mdr1a*(−/−) mice have demonstrated the functional importance of P-gp in limiting brain penetration of many drugs and have also established a role of Mdr1 in drug absorption and excretion into bile and urine (Schinkel et al., 1995, 1996; Schinkel, 1998; Jonker et al., 1999; Chen et al., 2003). *Mdr1a*(−/−) mice are a powerful tool for selecting non-P-gp substrates for central nervous system (CNS)-targeted drugs and establishing pharmacokinetic/pharmacodynamic relationships. Because rats are frequently used in the drug development process, a rat model lacking Mdr1a would serve as an additional valuable in vivo model.

In this study, we used ZFN technology to manipulate the rat *Mdr1a* gene. The resulting *Mdr1a*(−/−) rats were molecularly and pharmacologically characterized. Our results suggest that the Mdr1a rat KO model would serve as a valuable in vivo model for pharmacological studies.

Materials and Methods

Animals. *Mdr1a*(−/−) and wild-type Wistar Hannover rats (10–12 weeks old) were used. Animals were kept in a temperature-controlled environment with a 12-h light/dark cycle and received food and water ad libitum. All animal handling was according to Animal Procedure Statements approved by the Merck Rahway Institutional Animal Care and Use Committee.

Chemicals. Loperamide and indinavir were obtained from Sigma-Aldrich (St. Louis, MO). Talinolol was purchased from Toronto Research Chemicals Inc. (North York, ON, Canada). All other reagents were commercially obtained and of the highest analytical purity grade.

ZFN mRNA Preparation and Microinjections of Rat Embryos. ZFN constructs targeting the rat *Mdr1a* gene were designed and purchased from Sigma-Aldrich. The constructs have been described elsewhere (Carbery et al., 2010; Cui et al., 2010), and the targeting site is shown in Fig. 1. ZFN expression plasmids were linearized by XbaI site and transcribed using a MessageMax T7 kit and poly(A) tailing kit (Epicenter Technologies, Madison, WI) according to the manufacturer's protocol. The final products were purified using a MegaClean kit (Ambion, Austin, TX) and dissolved in water. RNA was quantified and adjusted to desired concentration (2 ng/μl) using Tris-EDTA buffer (10 mM Tris, pH 7.6, and 1 mM EDTA) for embryo injection.

All animal work was done in accordance with Merck institutional animal care guidelines. Wistar-Hannover rats purchased from Charles River Laboratories, Inc. (Wilmington, MA) were housed in standard conditions under a 14-h/10-h light/dark cycle. Four- to 5-week-old females were superovulated with 30 U of pregnant mare serum gonadotropin followed 48 h later by 40 U of human chorionic gonadotropin and placed with fertile males of the same strain. Fertilized oocytes were collected the next morning and microinjected with ZFN mRNA (2 ng/μl) into cytoplasm or pronucleus. Surviving oocytes were implanted into the oviducts of pseudopregnant Sprague-Dawley females and allowed to go to term.

Genomic DNA Preparation and Targeted Allele Identification. Rat genomic DNA was extracted from the tail tip using a Mammalian GenElute kit (Sigma-Aldrich) following the manufacturer's protocol. To detect small deletions generated by NHEJ, a Cel-1 assay was performed as described elsewhere using a Surveyor mutation detection kit (Carbery et al., 2010). The sequences of PCR primers of Mdr1a were TTGGCAAAACAAAACTGGCT and TTAGCAAAAAGCATGAAATTGTG.

Western Blot Analysis. Rat tissue samples were collected and snap-frozen in liquid nitrogen for future processing. Membrane fractions from different tissues were prepared using a Qproteome cell compartment kit (QIAGEN, Hilden, Germany) following the manufacturer's protocol. Then 20 to 30 μg of protein for each sample was loaded onto NuPAGE 4 to 12% SDS gel (Invitrogen, Carlsbad, CA) and transferred to a nitrocellulose membrane. Western blotting using anti-Mdr1a (C219; Abcam Inc., Cambridge, MA) or anti-actin (Cell Signaling Technology, Danvers, MA) antibodies was performed using a WesternBreeze chemiluminescent kit (Invitrogen) following the manufacturer's protocol.

Analysis of Serum and Urine. Male and female *Mdr1a*(−/−) and wild-type rats were used in this study. The animals were fasted overnight with free access to water before the study. Blood samples were taken by cardiac puncture. The serum samples obtained were used for analysis. Urine samples were collected overnight in metabolic cages. During urine collection, samples were kept on ice and in the dark. Serum and urine chemistry parameters were determined using a Hitachi 911 clinical chemistry analyzer (Roche Diagnostics, Indianapolis, IN). Sodium, potassium, and chloride levels were determined using ion-specific electrodes. Other tests were performed by standard biochemical methods.

Loperamide and Indinavir Brain Penetration Studies. Male *Mdr1a*(−/−) and wild-type rats were used in these studies. Loperamide was dissolved in saline containing 5% ethanol at a concentration of 0.2 mg/ml. Indinavir was dissolved in saline-propylene glycol-ethanol [50:40:10 (v/v)] at a concentration of 0.5 mg/ml. After intravenous administration of loperamide (1 mg/kg) or indinavir (2 mg/kg) via a catheterized femoral vein, three rats from each group were sacrificed at 0.5, 2, and 4 h, and plasma and brain samples were collected. All samples were kept at −80°C until LC-MS/MS analysis.

Talinolol Pharmacokinetic Studies. Male *Mdr1a*(−/−) and wild-type rats were used in these studies. The animals were fasted overnight with free access to water before the study. Talinolol, formulated in sodium phosphate buffer (0.2 M, pH 7.4)-propylene glycol-ethanol [40:40:20 (v/v)] or polyethylene glycol 400-ethanol-water [25:15:60 (v/v)], was administered via intravenous injection into a catheterized femoral vein (1 mg/kg) or oral gavage (5 mg/kg). Multiple blood samples were collected from the femoral artery at designated time points, and plasma samples were separated by centrifugation immediately. All samples were kept at −80°C until further analysis.

Quantitative RT-PCR and PCR Array for mRNA Analysis. RNA was isolated from tissues of *Mdr1a*(−/−) and wild-type male and female rats with three animals per group. Total RNA was isolated using an RNeasy kit from QIAGEN, and cDNA was synthesized using a High-Capacity cDNA Archive kit (Applied Biosystems, Foster City, CA) as described previously (Chu et al., 2006). TaqMan low-density microarray cards were custom-made by Applied Biosys-

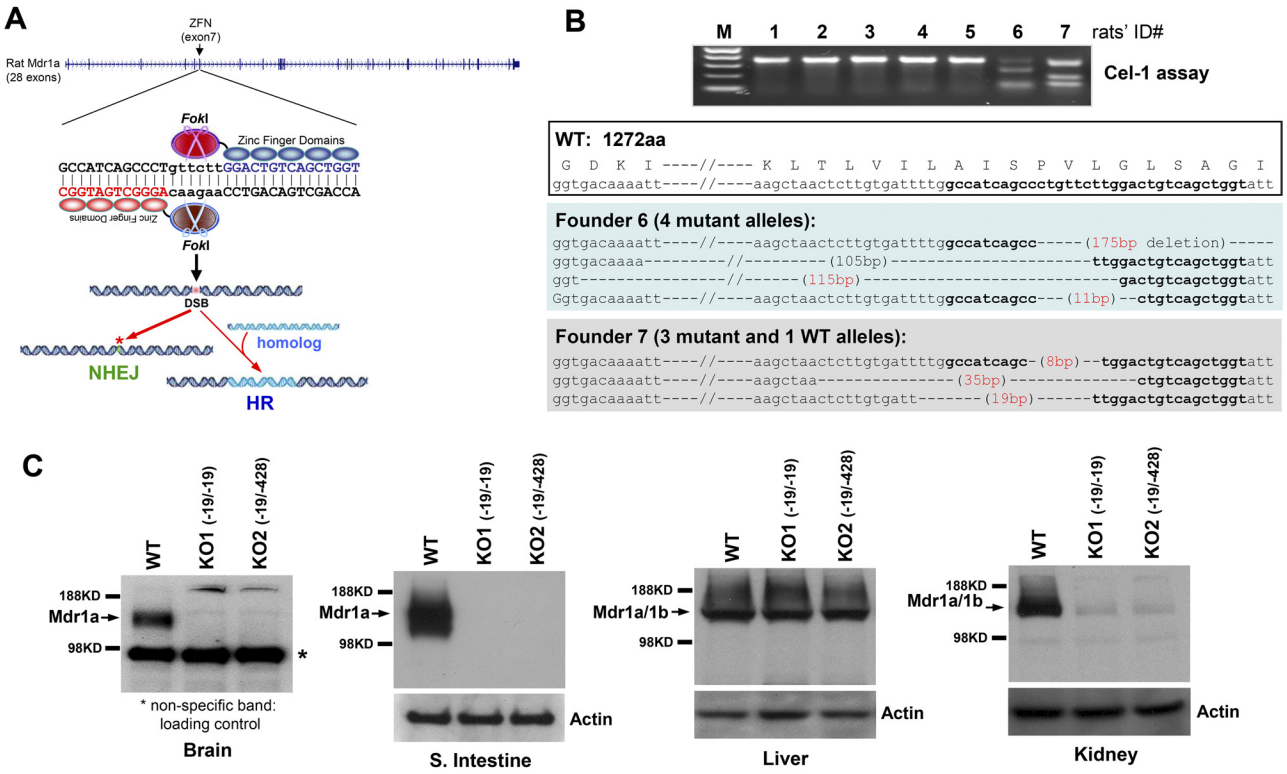

Fig. 1. Microinjection of *Mdr1a* ZFN mRNA into rat one-cell embryos specifically induces targeted gene mutations. A, schematic representations of the rat *Mdr1a* gene structure and the position of the ZFN targeting site selected. The two ZFN binding sequences are shown in opposite orientation in blue and red, respectively. The ZFN pair consists of two subunits, one with six and one with five fingers, respectively. When the ZFN pair binds to the target site, the two FokI domains dimerize to generate a DNA double-strand break (DSB), which will be repaired by either NHEJ (major) or HR (minor) pathways. B, screening and analyses of mutant alleles in the rat offspring derived from ZFN-injected embryos. The positive result in the Cel-1 assay indicates that six and seven pups may carry mutations near the Mdr1a ZFN target site. The genomic regions surrounding the ZFN site from founder 6 and 7 were cloned and sequenced. Founder 6 contains four mutant alleles, with 175-, 115-, 105-, and 11-bp deletions, respectively. Founder 7 contains one wild-type (WT) allele and three mutant alleles with 8-, 35-, and 19-bp deletions, respectively. The open reading frame of Mdr1a near the ZFN site is shown (1272 amino acids). The deletions that cause frameshift and translational premature termination are highlighted in red. C, Western blots showing undetectable levels of Mdr1a protein in the brain and small intestine (S. Intestine) of KO rats. In the liver sample, the band with a size that was apparently similar to that of the Mdr1a protein in KO rats may represent the up-regulated Mdr1b protein because of the cross-reactivity of the antibody. The weak potential Mdr1b protein was detected in the kidney of KO rats as well but not as strongly as in liver.

tems and contained probes for the detection of 90 genes (Supplemental Tables S1 and S2). Real-time quantitative PCR was performed using an ABI PRISM 7900 Sequence Detection System (Applied Biosystems). Changes in gene expression were determined by the ΔΔCt method (Livak and Schmittgen, 2001). The cycle threshold value (Ct) represents the PCR cycle at which the level of fluorescence during RT-PCR for a specific target gene exceeds the baseline threshold. Quantitation of the target cDNAs in all samples was normalized to 18S ribosomal RNA ($Ct_{target} - Ct_{18S} = \Delta Ct$), and the difference in expression for each target cDNA in the *Mdr1a*(−/−) rat was expressed to the amount in the wild-type rat ($\Delta Ct_{wild\text{-}type} - \Delta Ct_{Mdr1a(-/-)} = \Delta\Delta Ct$). Fold changes in target gene expression were determined by taking 2 to the power of this value ($2^{-\Delta\Delta Ct}$).

A 384-well format custom-designed PCR array was obtained from SABiosciences (Frederick, MD). The custom rat 384-well array was designed to combine four existing SABioscience 96-well arrays for Drug Metabolism and Transporters (Drug Metabolism: Phase I Enzymes, Drug Metabolism: Phase II Enzymes, Drug Transporters, and Drug Resistance and Metabolism PCR Array; http://www.sabiosciences.com/ArrayList.php?pline=PCRArray). A total of 372 genes and 5 housekeeping genes were assayed. Genomic DNA contamination primer control and positive PCR controls were all included on the array as part of SABiosciences standard array setup. Then 0.5 to 2 μg of total RNA from each sample was used in 50 μl of cDNA reaction by using a High-Capacity Archive cDNA kit. The cDNA reaction was set up in a Biomek FX liquid handling system, and 10 μl of the PCR was loaded into each well of the PCR array using a Biomek FX liquid handling system. Real-time PCR was performed on the 7900HT PCR system (Applied Biosystems) with 2× SYBR Fast PCR Master Mix (SABiosciences) and 2 μl of cDNA for each reaction. The expression levels of mRNA for each gene were normalized to the average of *Actb*, *Hprt1*, *Ldha*, *Rplp1*, and *Rp113a* in each sample. Genes with greater than 2-fold changes were further validated by individual TaqMan (Applied Biosystems) qRT-PCR.

Quantification of Loperamide, Indinavir, and Talinolol in Plasma and Brain Samples. Plasma samples were thawed on ice. A 50-μl sample was taken, and 6 volumes of acetonitrile containing 100 nM alprazolam or 40 ng/ml labetalol (Sigma-Aldrich) as internal standard were added to the samples and standard solutions. After mixing, the contents were centrifuged at 1800*g* for 10 min. The supernatant was then transferred to a 96-well plate and analyzed using liquid chromatography-tandem mass spectrometry. Brain samples were weighed and placed in a 20-well plate, and a 2-fold amount of water and four stainless steel beads were added. The brains were then homogenized using the 2000 Geno/Grinder (Spex CertiPrep, Metuchen, NJ). A 100- to 150-μl sample of the homogenate of each brain sample was taken and placed in a 96-well plate and analyzed by LC-MS/MS. Chromatography was performed using an Atlantis T3 column (2.1 × 50 mm, 3-μm particle size; Waters, Milford, MA) and an HPLC system consisting of Transcend System pumps and an LX-2 (with an Aria OS 1.61 operating system) autosampler (Thermo Fisher Scientific, Waltham, MA), using a gradient of water with 0.1% formic acid (A) and acetonitrile with 0.1% formic acid (B). The HPLC flow rate was 0.7 to 0.75 ml/min. Before

the gradient was begun, the mobile phase was 5% B for 15 s. The gradient was then started with 5 or 10% B going to 90 or 95% B over 60 or 90 s. The mobile phase was 90 or 95% B for 25 s after which it was returned to 5 or 10% B for 50 or 60 s. Detection of the loperamide and talinolol was performed using a Sciex API 5000 mass spectrometer (MDS Sciex, Toronto, ON, Canada), and detection of indinavir was performed using a Sciex API 4000 mass spectrometer (MDS Sciex) in the positive ion mode using the TurboIonSpray source. Mass transition (*m/z*) monitoring for loperamide, talinolol, and indinavir was 477.2 to 266.2, 364.1 to 100.4, and 614.2 to 465.4, respectively. The concentration of test compound in plasma or brain samples was determined by comparing the test compound with internal standard peak area ratios against a standard curve. The lower limit of quantification in both matrices was 0.5 ng/ml (talinolol) and 1 ng/ml (loperamide). All quality controls were within 20 to 25% of the nominal value.

Determination of Pharmacokinetic Parameters. Pharmacokinetic parameters of talinolol were calculated using Watson software (version 6) with noncompartmental models.

Statistical Analysis. Student's *t* tests were used to determine the significance of differences between groups of animals. Differences with $P < 0.05$ were considered significant.

Results

Generation of *Mdr1a* KO Rats Using a Sequence-Specific ZFN. A pair of ZFNs was designed and generated by Sigma-Aldrich to target the rat *Mdr1a* gene (Carbery et al., 2010; Cui et al., 2010). The ZFN target site resides in Mdr1a exon 7 (Fig. 1A). The ZFN was initially tested in rat C6 cells (Supplemental Fig. S1), showing that it specifically targeted the *Mdr1a* gene with high efficiency but not the closely related *Mdr1b* gene. To test ZFN activity in rats, the mRNAs encoding Mdr1a ZFNs were directly injected into the pro-nuclei or cytoplasm of one-cell embryos. The resulting pups were genotyped by the Cel-1 assay or direct PCR using genomic DNA isolated from tails. As shown in Fig. 1B, two of seven pups contained mutations near the ZFN target site. The mutant alleles from the two founders were cloned and sequenced. Of interest, multiple mutant alleles were identified in these founders including four in founder 6 and three in founder 7 (Fig. 1B). This mosaic nature of the founders generated by ZFN is consistent with previous reports (Geurts et al., 2009; Carbery et al., 2010; Cui et al., 2010; Mashimo et al., 2010) and suggests that the activity of the ZFN can persist beyond the one-cell stage of embryogenesis. Among the 66 live-born offspring, 22 (~33%) positive founders carrying mutant alleles were identified (Supplemental Table S1). Moreover, analyses of rat genomic regions that shared high homology (with four or five mismatches) to the Mdr1a ZFN site did not detect any off-target cleavage (Supplemental Fig. S2).

Mdr1a(−/−) rats displayed normal development, viability, and fertility, without obvious differences from wild-type rats in terms of body weight and fecal matter. In general, serum and urine chemistry parameters were comparable in *Mdr1a*(−/−) rats and in controls, except for a 2.2-fold lower urine calcium level in male KO compared with wild-type, a 1.7-fold higher urine calcium level in female KO compared with wild-type, and a 3.5-fold lower urine protein level in KO female compared with wild-type animals (data not shown).

Detection of Mdr1 by Western Blotting. To confirm that the ZFN-generated mutations resulted in nondetectable levels of the Mdr1a protein, we characterized the homozygous *Mdr1a*(−/−) rats by Western blotting. Membrane fractions from wild-type and *Mdr1a*(−/−) rat brain, small intestine, liver, and kidney were analyzed using the anti-Mdr1a antibody C219. Two KO rats were examined. KO1 carries two identical 19-bp deletion alleles. KO2 carries one 19-bp deletion and one 428-bp deletion allele. As shown in Fig. 1C, the Mdr1a protein was completely absent in both brain and small intestines of the two *Mdr1a*(−/−) rat strains analyzed. Because C219 also cross-reacts with Mdr1b, the Western blots demonstrated that Mdr1b expression was still present in liver and kidney. This was especially the case in liver where Mdr1b is probably up-regulated upon inactivation of the *Mdr1a* gene (see below and Fig. 1C). Because no difference between the two deletion alleles (19 and 428 bp) characterized was detected, all subsequent studies were conducted using the homozygous strain with the 19-bp deletion in Mdr1a exon 7.

Brain Penetration of Loperamide and Indinavir in *Mdr1a*(−/−) Rats. To confirm the functional absence of Mdr1a in *Mdr1a*(−/−) rats, brain penetration of loperamide and indinavir, two previously validated substrates for human MDR1 and rodent Mdr1a (Schinkel et al., 1996; Kim et al., 1998; Choo et al., 2000), was investigated in *Mdr1a*(−/−) and wild-type rats. After intravenous administration of loperamide, the brain concentration of loperamide in *Mdr1a*(−/−) rats was 22- to 107-fold higher (at 0.5, 2, and 4 h, $P < 0.05$) than that in control rats (Fig. 2A), whereas the plasma concentration time profile of loperamide in *Mdr1a*(−/−) rats was 1.3- to 2-fold higher than that in wild-type rats (at 0.5, 2, and 4 h, $P < 0.05$) (Fig. 2B). The brain/plasma concentration ratio ($K_{p,\,brain}$) in wild-type rats ranged from 0.36 to 0.42, whereas the ratio in *Mdr1a*(−/−) rats was time-dependent and increased from 7- to 23-fold (at 0.5, 2, and 4 h, $P < 0.05$) (Fig. 2C), indicating a loss of function of Mdr1a in the brain of *Mdr1a*(−/−) rats. Furthermore, because loperamide is an opioid-receptor agonist, a pronounced opiate-like CNS effect were observed in the *Mdr1a*(−/−) rats, such as weak breathing, immobility, and no blink reflex. Similar to that for loperamide, the indinavir brain concentration in *Mdr1a*(−/−) rats was significantly higher than that in wild-type rats at all time points tested ($P < 0.05$) (Fig. 2D), whereas there was no significant difference in the plasma concentration-time profile (Fig. 2E). The $K_{p,\,brain}$ of indinavir in wild-type rats was time-dependent and increased from 0.5 to 2.6, whereas $K_{p,\,brain}$ in *Mdr1a*(−/−) rats increased from 6.4 to 77.2 (at 0.5 and 2 h, $P < 0.05$) (Fig. 2F).

Pharmacokinetics of Talinolol in *Mdr1a*(−/−) Rats. To assess the effect of Mdr1a on the intestinal absorption and pharmacokinetics of talinolol, a substrate for human and rat P-gp and organic anion-transporting polypeptides (OATPs) (Shirasaka et al., 2009, 2010), we administered talinolol orally or intravenously to wild-type and *Mdr1a*(−/−) rats and subsequently determined the plasma concentration-time profile (Fig. 3, A and B). Analysis of the pharmacokinetic parameters showed that the area under the curve ($AUC_{0-\infty}$) and plasma clearance in *Mdr1a*(−/−) were comparable with those in wild-type rats after intravenous administration, whereas the $AUC_{0-\infty}$ in *Mdr1a*(−/−) rats was increased 4.5-fold ($P < 0.05$) after oral administration (Table 1). The bioavailability of talinolol in *Mdr1a*(−/−) and wild-type rats was 23 and 7%, respectively (Table 1).

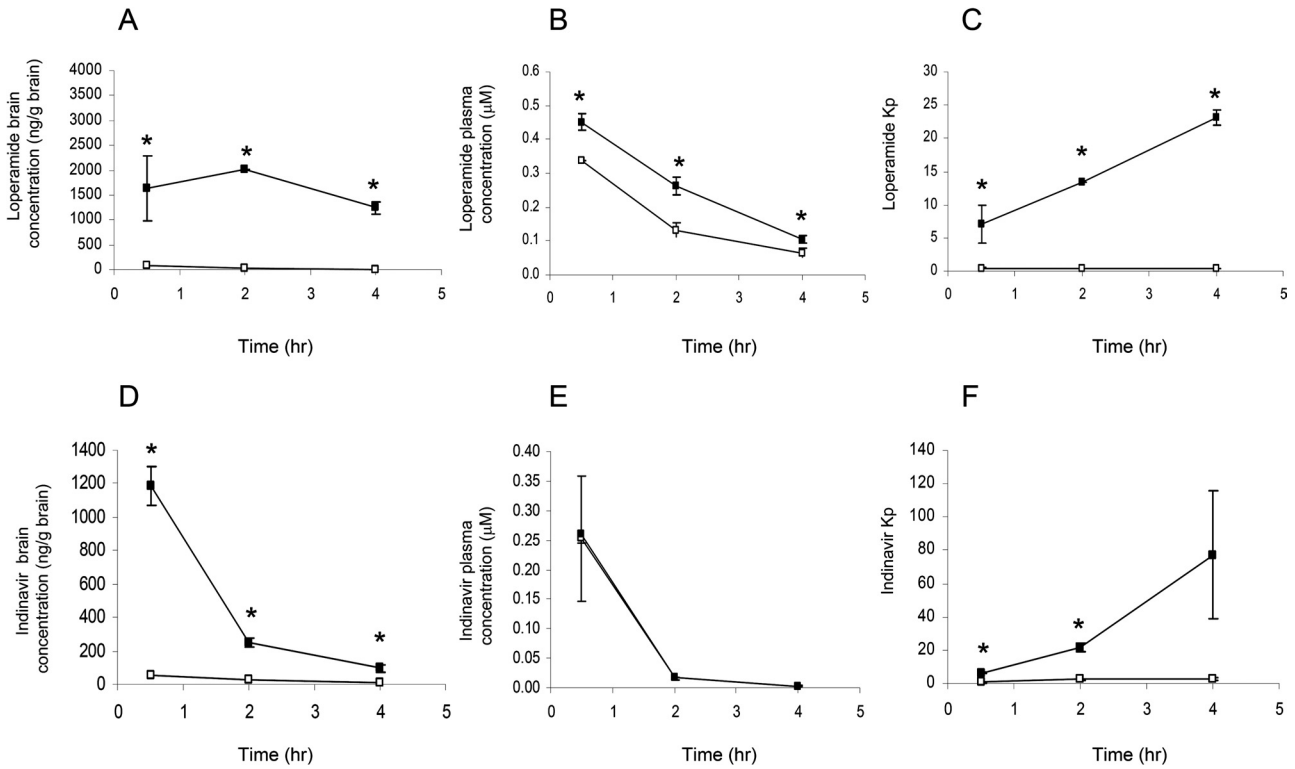

Fig. 2. Brain and plasma concentrations of loperamide and indinavir in *Mdr1a*(−/−) and wild-type rats. After intravenous injection of loperamide (1 mg/kg) or indinavir (2 mg/kg), *Mdr1a*(−/−) (■) and wild-type rats (□) were sacrificed at the indicated time points. The brain and plasma concentrations of loperamide (A and B) and indinavir (D and E) were measured by LC-MS/MS. $K_{p,\ brain}$ values of loperamide (C) and indinavir (F) were also estimated. Values shown are means ± S.E. ∗, significantly different from wild-type animals ($P < 0.05$).

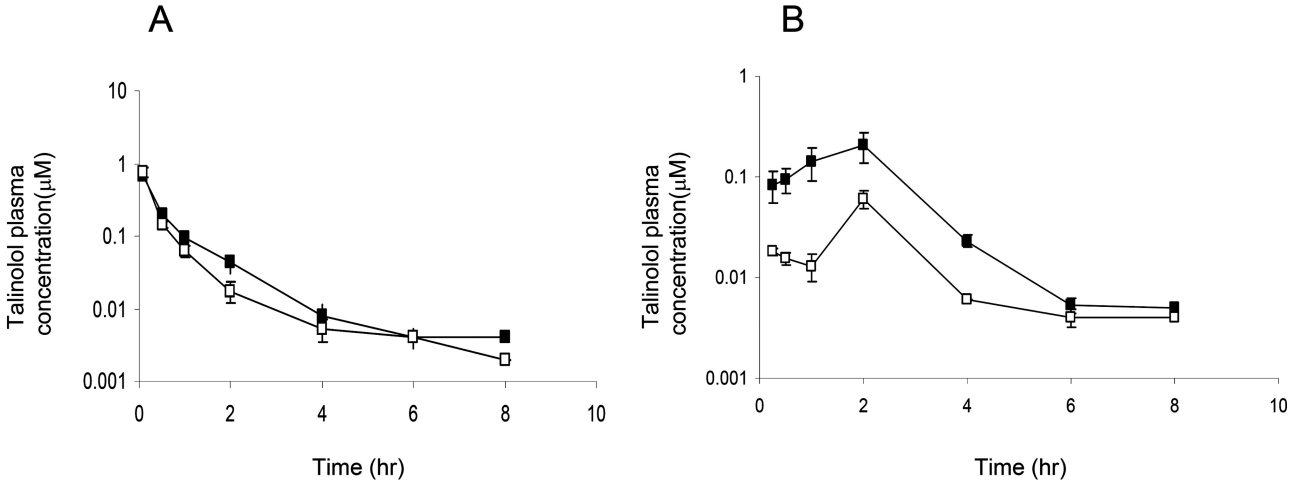

Fig. 3. Plasma concentrations of talinolol in *Mdr1a*(−/−) and wild-type rats after intravenous and oral administration. Plasma concentrations of talinolol in *Mdr1a*(−/−) (■) and wild-type rats (□) were measured by LC-MS/MS after intravenous (1 mg/kg) (A) and oral (5 mg/kg) (B) administration of talinolol. Values shown are means ± S.E.

Gene Expression Profiling in Brain, Intestine, Liver, and Kidney. To investigate whether the loss of Mdr1a alters the expression profile of other drug transporters and metabolizing enzymes, we used 96-well TaqMan Low-Density Microarrays (Micro Fluidic Cards) and 384-well PCR arrays (SABiosciences) to determine expression changes in brain, intestine, liver, and kidney of wild-type and *Mdr1a*(−/−) female and male rats. The genes in the 384-well PCR array included the 90 phase I and II drug-metabolizing enzymes and transporters in the TaqMan Low-Density Microarray as well as an additional 282 drug metabolism and transporter genes (Supplemental Tables S2–S4). The genes with significant changes observed from the 372-gene panel (Supplemental Tables S2 and S3; Supplemental Figure S3) were further validated by individual TaqMan qRT-PCR. The genes that showed ≥2-fold up- or down-regulation ($P < 0.05$), on the basis of TaqMan qRT-PCR, in *Mdr1a*(−/−) rats compared with wild-type animals in liver, intestine, kidney, and brain are presented in Fig. 4.

The amount of Mdr1a (*Abcb1a*) mRNA was 5- to 50-fold lower in brain, liver, kidney, and intestine of *Mdr1a*(−/−) rats than in wild-type rats. The lower transcript level of

TABLE 1
Pharmacokinetic parameters of talinolol in Mdr1a(−/−) and wild-type rats after intravenous (1 mg/kg) and oral (5 mg/kg) administration of talinolol

Parameters	Intravenous		Oral	
	WT	*Mdr1a*(−/−)	WT	*Mdr1a*(−/−)
AUC/dose, μM · h/mg/kg	0.3 ± 0.06	0.4 ± 0.05	0.02 ± 0.002	0.09 ± 0.02*
$t_{1/2}$, h	0.7 ± 0.2	1.0 ± 0.2		
Cl, ml · min^{-1} · kg^{-1}	153 ± 18	119 ± 15		
Vd_{ss}, l/kg	4.8 ± 0.5	6.5 ± 1.3		
C_{max}, μM			0.06 ± 0.01	0.21 ± 0.07
T_{max}, h			2.0 ± 0.00	1.7 ± 0.3
F, %			7	23

WT, wild-type; Cl, clearance; Vd_{ss}, volume of distribution at steady state; C_{max}, maximum concentration; T_{max}, time to reach maximum concentration; F, bioavailability.
* Significantly different from wild-type animals ($P < 0.05$).

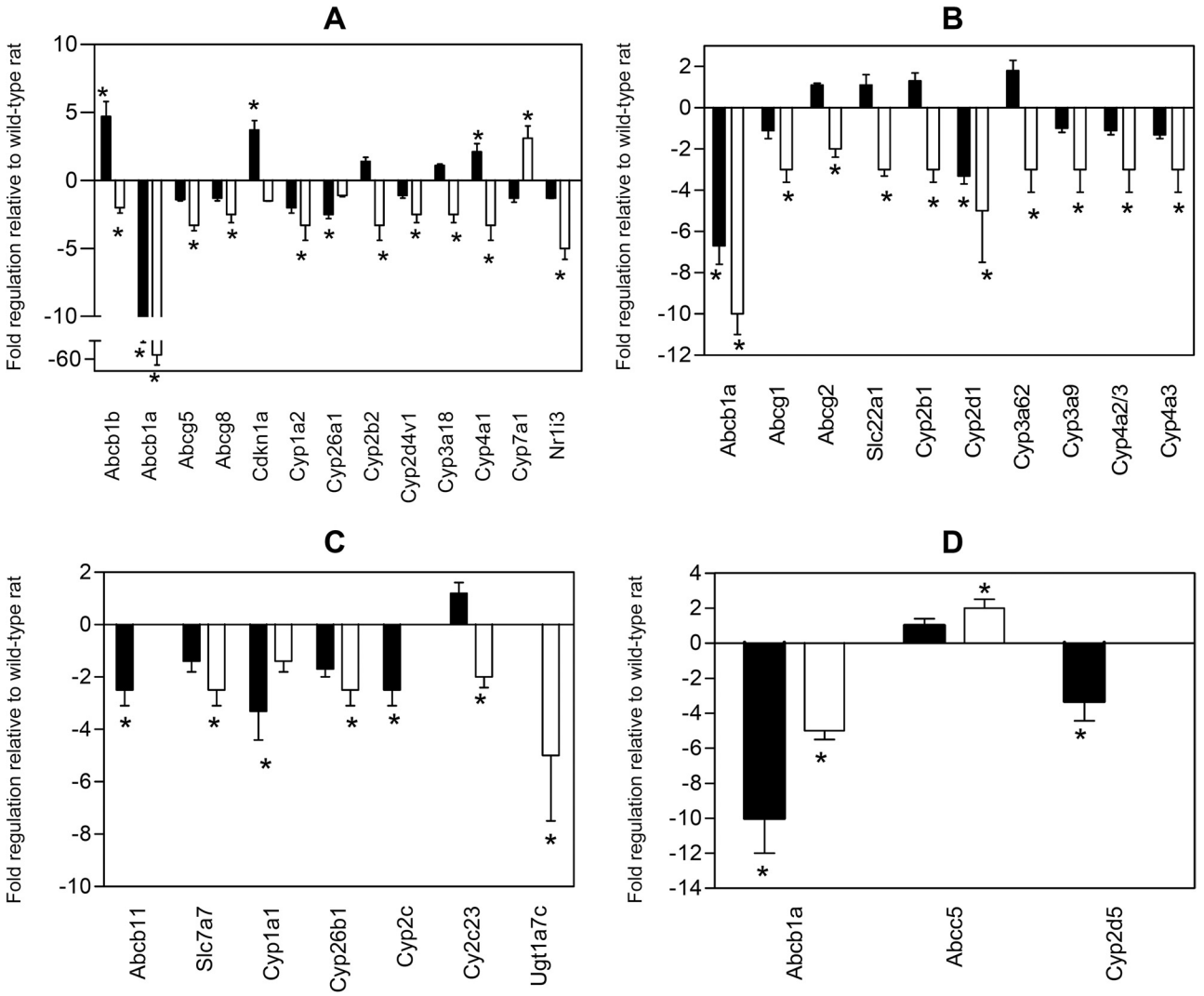

Fig. 4. Gene expression of various transporters and drug-metabolizing enzymes in *Mdr1a*(−/−) rat brain, liver, intestine, and kidney compared with controls. From 90 genes tested, the expression of the genes that showed ≥2-fold up- or down-regulation (*, $P < 0.05$) in *Mdr1a*(−/−) rats compared with that in wild-type animals in liver (A), intestine (B), kidney (C), and brain (D) is presented. The data are expressed as the fold regulation relative to that in wild-type rats. Fold change greater than 1 indicates up-regulation, and the fold regulation is equal to fold change. Fold change less than 1 indicates down-regulation, and the fold regulation is the negative inverse of the fold change. ■, male rats; □, female rats. The data represent mean values of three independent experiments.

Mdr1a mRNA probably resulted from nonsense-mediated mRNA decay because the deletion in exon 7 caused the generation of multiple downstream premature termination codons. Similar to a previous report in *Mdr1a*(−/−)*/1b*(−/−) mice (Schinkel et al., 1997), Mdr1b (*Abcb1b*) gene expression was low in brain and intestine of both *Mdr1a*(−/−) and wild-type rats. If interest, Mdr1b was 4.7-fold higher and 2-fold lower in the liver of male and female *Mdr1a*(−/−) rats, respectively, whereas its expression in kidney of both male and female *Mdr1a*(−/−) rats was not changed compared with

that for controls. In female but not in male *Mdr1a*(−/−) rats, a 2-fold up-regulation of multidrug resistance protein 5 (*Abcc5*) in brain and a 2- to 2.5-fold lower expression of *Abcg1*, organic cation transporter 1 (*Slc22a1*), and Bcrp (*Abcg2*) in intestine was observed. In addition, *Abcg5* and *Abcg8* in liver of female *Mdr1a*(−/−) rats were 2.5- to 3-fold lower than those in wild-type animals. No significant differences were detected for any of the other transporter genes analyzed.

Of the cytochrome P450 and nuclear receptor genes analyzed, the expression of Cyp3a1/Cyp3a23 in liver of both male and female *Mdr1a*(−/−) rats was not changed compared with that in wild-type rats. In female *Mdr1a*(−/−) liver, the expression of Cyp1a2, Cyp2b2, Cyp2d4v1, Cyp3a18, and Cyp4a1 and the constitutive androstane receptor (Nr1i3) was 2.5- to 5-fold lower than that in controls, whereas Cyp7a1 was 3-fold higher than that in controls. In male *Mdr1a*(−/−) liver, Cyp26a1 and Cyp4a1 were expressed 2.5-fold lower and 2-fold higher than in wild-type rats, respectively. The Cyp3a9 and Cyp3a62 enzymes, which contribute to intestinal drug metabolism in rats (Aiba et al., 2005), were 3-fold lower in female *Mdr1a*(−/−) rats. The expression of Cyp2d1 was 3- to 5-fold lower in intestine of both male and female *Mdr1a*(−/−) rats. In kidney, expression of Cyp1a1 and Cyp26b1 was 2.5- to 3-fold lower in male and female *Mdr1a*(−/−) rats, respectively.

For the UDP-glucuronosyltransferase and sulfotransferase genes analyzed, Sult1a1 was 3-fold lower in the intestine of male *Mdr1a*(−/−) rats. Ugt1a7c was 5-fold lower in kidney of female *Mdr1a*(−/−) rats. The 3.7-fold up-regulation of the *Cdkn1a* (cyclin-dependent kinase inhibitor 1) gene was observed in male *Mdr1a*(−/−) rats.

Discussion

We have generated an *Mdr1a*(−/−) rat model using ZFN-mediated gene targeting through NHEJ pathways with high efficiency. The *Mdr1a*(−/−) rats are healthy and show no obvious phenotypic abnormalities. Western blots confirmed that no Mdr1a was present in brain and intestine. A signal was still detectable in kidney and liver, explained by the cross-reactivity of the antibody used with Mdr1b. The functional absence of Mdr1a was demonstrated by a significant increase in brain penetration of loperamide and indinavir and the intestinal absorption of talinolol in the *Mdr1a*(−/−) rats.

A general concern in the use of transporter knockout animals for pharmacokinetic studies is the potential compensatory effect from up- or down-regulation of other transporters and drug metabolism-related genes, which may complicate the interpretation of data obtained with such animals. As reported by Schinkel et al. (1994) in *Mdr1a*(−/−) mice, the expression of Mdr1b was higher in the liver of male and female mice and the kidney of male mice as well. Our studies showed that Mdr1b RNA was up-regulated 4.7-fold only in the liver of male *Mdr1a*(−/−) rats, whereas the expression of Mdr1b in kidney of both male and female *Mdr1a*(−/−) rats was unchanged. Because the anti-Mdr1a antibody used in Western blot analysis cross-reacts with the Mdr1b protein, high expression of Mdr1 detected in the male *Mdr1a*(−/−) liver is probably due to the up-regulation of Mdr1b. In the intestine of female *Mdr1a*(−/−) rats, the expression of Bcrp, which may contribute to intestinal secretion of its substrates, was ~50% lower compared with that in wild-type animals. However, it is not clear whether such changes at the level of mRNA levels will translate into the change at the Bcrp protein level. We were not able to test this by Western blot analysis because of the unavailability of very selective Bcrp antibodies (data not shown).

In general, alterations in gene expression of phase I and II drug-metabolizing enzymes in *Mdr1a*(−/−) rats seemed to be modest, with more changes in female rats. For instance, hepatic expression of the constitutive androstane receptor, one of major nuclear receptors responsible for regulating many absorption, distribution, metabolism, and excretion-related genes was 5-fold lower in female *Mdr1a*(−/−) rats. The mechanism for such down-regulation is not clear. Numerous studies have suggested that CYP3A and P-gp work synergistically in limiting the systematic exposure of orally administered drugs (Benet et al., 1999). In female *Mdr1a*(−/−) rats, the mRNA expression of Cyp3a9 and Cyp3a62 in intestine was 3-fold lower than that in wild-type rats. Although further studies are needed to confirm that these changes are resulting in altered enzyme activity, caution should be exercised in interpreting pharmacokinetic data obtained in female *Mdr1a*(−/−) rats that are substrates for Cyp3a9 or Cyp3a62.

One of the major applications of *Mdr1a*(−/−) rats will be studying the role of P-gp in brain penetration of drugs, which has been critical for selecting CNS-targeted drugs or reducing CNS toxicity for non-CNS drugs. Our findings demonstrate that *Mdr1a*(−/−) rats are a sensitive model to measure the role of P-gp in brain penetration. Similar to the reports in *Mdr1a*(−/−) mice (Schinkel et al., 1996; Kim et al., 1998), a significant increase in the brain penetration of loperamide and indinavir was observed in *Mdr1a*(−/−) rats. $K_{p,\,brain}$ in KO versus wild-type rats was 17- to 63-fold for loperamide and 9- to 30-fold for indinavir, respectively. This value is higher than that previously reported for *Mdr1a*(−/−) mice. The cause of this discrepancy is possibly the difference in analytical methods applied, because we measured $K_{p,\,brain}$ of the parent drugs loperamide or indinavir by LC-MS/MS, whereas only total radioactivity was measured in the experiments with *Mdr1a*(−/−) mice. As an alternative, the possibility that the activity of P-gp in the brain of rat is higher than that in mouse cannot be ruled out.

In addition to brain penetration, *Mdr1a*(−/−) rats will be a useful tool to study the role of P-gp in limiting intestinal drug absorption. Talinolol, a clinically used β_1 selective adrenergic antagonist, is a substrate for P-gp and OATPs (Shirasaka et al., 2009, 2010) and is not metabolized by CYP3A4. The overall metabolic clearance of talinolol is low, and 99% of the drug is eliminated unchanged (Trausch et al., 1995). The pharmacokinetics of talinolol after oral administration are nonlinear, and the extent of absorption is highly dependent on the dose level (Kagan et al., 2010), which might be attributed to saturation of P-gp-mediated intestinal efflux. Our studies showed that the plasma AUC of talinolol in *Mdr1a*(−/−) rats increased 4.5-fold compared with that in wild-type animals after oral administration (5 mg/kg), whereas P-gp did not have a significant effect on the plasma AUC of talinolol after intravenous dosing. Therefore, these data suggest that rat Mdr1a plays a significant role in limiting the intestinal absorption of talinolol. Of interest, the oral bioavailability of talinolol in humans is much higher

than that in rats (~55% in humans at a 100-mg dose versus 7% in rats at 5 mg/kg), although the dose level in rats in our study was higher than that in humans (Trausch et al., 1995). This finding is probably due to potential species differences in the functional activity of MDR1/Mdr1a and OATPs between human and rats. Further investigations are needed to confirm this hypothesis.

ZFN-mediated direct gene KO in rat embryos has recently been proven to be successful in numerous reports (Geurts et al., 2010; Mashimo et al., 2010; Ménoret et al., 2010). However, genetic modification of target genes through HR is critical to enable engineering of the rat genome in a flexible way. A recent report has demonstrated the feasibility of achieving HR directly in rat embryo facilitated by ZFN (Cui et al., 2010), which may expand the application of this technology and allow the generation of conditional KO/knock-in or humanized rat models. The robustness and full utility of this advancement need to be explored further.

Acknowledgments

We thank Xiaoli Ping, Loise Gichuru, Nina Jochnowitz, Chris Loewrigkeit, Carol Ann Keohane, and Alexandra Wickham for providing surgical support. Thanks to Irene Capodanno, Christian N. Nunes, and Pan Yi for technical assistance. We also thank Merck Research Laboratories New Technology Review and Licensing Committee.

Authorship Contributions

Participated in research design: Chu, Zhang, Vogt, Evers, and Shin.

Conducted experiments: Chu, Zhang, Yabut, Horwitz, Levorse, Xiang-qing Li, Zhu, Lederman, Ortiga, Strauss, Xiaofang Li, Owens, and Dragovic.

Performed data analysis: Chu, Zhang, Yabut, Evers, and Shin.

Wrote or contributed to the writing of the manuscript: Chu, Zhang, Vogt, Evers, and Shin.

References

Aiba T, Yoshinaga M, Ishida K, Takehara Y, and Hashimoto Y (2005) Intestinal expression and metabolic activity of the CYP3A subfamily in female rats. *Biol Pharm Bull* **28:**311–315.

Aitman TJ, Critser JK, Cuppen E, Dominiczak A, Fernandez-Suarez XM, Flint J, Gauguier D, Geurts AM, Gould M, Harris PC, et al. (2008) Progress and prospects in rat genetics: a community view. *Nat Genet* **40:**516–522.

Benet LZ, Izumi T, Zhang Y, Silverman JA, and Wacher VJ (1999) Intestinal MDR transport proteins and P-450 enzymes as barriers to oral drug delivery. *J Control Release* **62:**25–31.

Capecchi MR (2005) Gene targeting in mice: functional analysis of the mammalian genome for the twenty-first century. *Nat Rev Genet* **6:**507–512.

Carbery ID, Ji D, Harrington A, Brown V, Weinstein EJ, Liaw L, and Cui X (2010) Targeted genome modification in mice using zinc-finger nucleases. *Genetics* **186:** 451–459.

Chen C, Liu X, and Smith BJ (2003) Utility of Mdr1-gene deficient mice in assessing the impact of P-glycoprotein on pharmacokinetics and pharmacodynamics in drug discovery and development. *Curr Drug Metab* **4:**272–291.

Choo EF, Leake B, Wandel C, Imamura H, Wood AJ, Wilkinson GR, and Kim RB (2000) Pharmacological inhibition of P-glycoprotein transport enhances the distribution of HIV-1 protease inhibitors into brain and testes. *Drug Metab Dispos* **28:**655–660.

Chu XY, Strauss JR, Mariano MA, Li J, Newton DJ, Cai X, Wang RW, Yabut J, Hartley DP, Evans DC, et al. (2006) Characterization of mice lacking the multidrug resistance protein Mrp2 (Abcc2). *J Pharmacol Exp Ther* **317:**579–589.

Cui X, Ji D, Fisher DA, Wu Y, Briner DM, and Weinstein EJ (2010) Targeted integration in rat and mouse embryos with zinc-finger nucleases. *Nat Biotechnol* **29:**64–67.

Devault A and Gros P (1990) Two members of the mouse mdr gene family confer multidrug resistance with overlapping but distinct drug specificities. *Mol Cell Biol* **10:**1652–1663.

Eyal S, Hsiao P, and Unadkat JD (2009) Drug interactions at the blood-brain barrier: fact or fantasy? *Pharmacol Ther* **123:**80–104.

Geurts AM, Cost GJ, Freyvert Y, Zeitler B, Miller JC, Choi VM, Jenkins SS, Wood A, Cui X, Meng X, Vincent A, Lam S, Michalkiewicz M, Schilling R, Foeckler J, Kalloway S, Weiler H, Ménoret S, Anegon I, Davis GD, Zhang L, Rebar EJ, Gregory PD, Urnov FD, Jacob HJ, and Buelow R.. (2009) Knockout rats via embryo microinjection of zinc-finger nucleases. *Science* **325(5939):**433.

Geurts AM, Cost GJ, Rémy S, Cui X, Tesson L, Usal C, Ménoret S, Jacob HJ, Anegon I, and Buelow R (2010) Generation of gene-specific mutated rats using zinc-finger nucleases. *Methods Mol Biol* **597:**211–225.

Geurts AM and Moreno C (2010) Zinc-finger nucleases: new strategies to target the rat genome. *Clin Sci* (*Lond*) **119:**303–311.

Hamra FK. (2010) Gene targeting: enter the rat. *Nature* **467:**161–163.

Giacomini KM, Huang SM, Tweedie DJ, Benet LZ, Brouwer KL, Chu X, Dahlin A, Evers R, Fischer V, Hillgren KM, et al. (2010) Membrane transporters in drug development. *Nat Rev Drug Discov* **9:**215–236.

Jonker JW, Wagenaar E, van Deemter L, Gottschlich R, Bender HM, Dasenbrock J, and Schinkel AH (1999) Role of blood-brain barrier P-glycoprotein in limiting brain accumulation and sedative side-effects of asimadoline, a peripherally acting analgaesic drug. *Br J Pharmacol* **127:**43–50.

Juliano RL and Ling V (1976) A surface glycoprotein modulating drug permeability in Chinese hamster ovary cell mutants. *Biochim Biophys Acta* **455:**152–162.

Kagan L, Dreifinger T, Mager DE, and Hoffman A (2010) Role of p-glycoprotein in region-specific gastrointestinal absorption of talinolol in rats. *Drug Metab Dispos* **38:**1560–1566.

Kim RB, Fromm MF, Wandel C, Leake B, Wood AJ, Roden DM, and Wilkinson GR (1998) The drug transporter P-glycoprotein limits oral absorption and brain entry of HIV-1 protease inhibitors. *J Clin Invest* **101:**289–294.

Kimura Y, Morita SY, Matsuo M, and Ueda K (2007) Mechanism of multidrug recognition by MDR1/ABCB1. *Cancer Sci* **98:**1303–1310.

Klug A (2010) The discovery of zinc fingers and their applications in gene regulation and genome manipulation. *Annu Rev Biochem* **79:**213–231.

Le Provost F, Lillico S, Passet B, Young R, Whitelaw B, and Vilotte JL (2010) Zinc finger nuclease technology heralds a new era in mammalian transgenesis. *Trends Biotechnol* **28:**134–141.

Lee CA, Cook JA, Reyner EL, and Smith DA (2010) P-glycoprotein related drug interactions: clinical importance and a consideration of disease states. *Expert Opin Drug Metab Toxicol* **6:**603–619.

Livak KJ and Schmittgen TD (2001) Analysis of relative gene expression data using real-time quantitative PCR and the $2^{-\Delta\Delta C_T}$ method. *Methods* **25:**402–408.

Mahar Doan KM, Humphreys JE, Webster LO, Wring SA, Shampine LJ, Serabjit-Singh CJ, Adkison KK, and Polli JW (2002) Passive permeability and P-glycoprotein-mediated efflux differentiate central nervous system (CNS) and non-CNS marketed drugs. *J Pharmacol Exp Ther* **303:**1029–1037.

Mashimo T, Takizawa A, Voigt B, Yoshimi K, Hiai H, Kuramoto T, and Serikawa T (2010) Generation of knockout rats with X-linked severe combined immunodeficiency (X-SCID) using zinc-finger nucleases. *PLoS One* **5:**e8870.

Ménoret S, Iscache AL, Tesson L, Rémy S, Usal C, Osborn MJ, Cost GJ, Brüggemann M, Buelow R, and Anegon I (2010) Characterization of immunoglobulin heavy chain knockout rats. *Eur J Immunol* **40:**2932–2941.

Miller DS, Bauer B, and Hartz AM (2008) Modulation of P-glycoprotein at the blood-brain barrier: opportunities to improve central nervous system pharmacotherapy. *Pharmacol Rev* **60:**196–209.

Raub TJ (2006) P-glycoprotein recognition of substrates and circumvention through rational drug design. *Mol Pharm* **3:**3–25.

Schinkel AH (1998) Pharmacological insights from P-glycoprotein knockout mice. *Int J Clin Pharmacol Ther* **36:**9–13.

Schinkel AH and Jonker JW (2003) Mammalian drug efflux transporters of the ATP binding cassette (ABC) family: an overview. *Adv Drug Deliv Rev* **55:**3–29.

Schinkel AH, Smit JJ, van Tellingen O, Beijnen JH, Wagenaar E, van Deemter L, Mol CA, van der Valk MA, Robanus-Maandag EC, and te Riele HP (1994) Disruption of the mouse *mdr1a* P-glycoprotein gene leads to a deficiency in the blood-brain barrier and to increased sensitivity to drugs. *Cell* **77:**491–502.

Schinkel AH, Wagenaar E, Mol CA, and van Deemter L (1996) P-glycoprotein in the blood-brain barrier of mice influences the brain penetration and pharmacological activity of many drugs. *J Clin Invest* **97:**2517–2524.

Schinkel AH, Wagenaar E, van Deemter L, Mol CA, and Borst P (1995) Absence of the mdr1a P-glycoprotein in mice affects tissue distribution and pharmacokinetics of dexamethasone, digoxin, and cyclosporin A. *J Clin Invest* **96:**1698–1705.

Shirasaka Y, Kuraoka E, Spahn-Langguth H, Nakanishi T, Langguth P, and Tamai I (2010) Species difference in the effect of grapefruit juice on intestinal absorption of talinolol between human and rat. *J Pharmacol Exp Ther* **332:**181–189.

Shirasaka Y, Li Y, Shibue Y, Kuraoka E, Spahn-Langguth H, Kato Y, Langguth P, and Tamai I (2009) Concentration-dependent effect of naringin on intestinal absorption of β_1-adrenoceptor antagonist talinolol mediated by P-glycoprotein and organic anion transporting polypeptide (Oatp). *Pharm Res* **26:**560–567.

Tong C, Li P, Wu NL, Yan Y, and Ying QL. (2010) Production of p53 gene knockout rats by homologous recombination in embryonic stem cells. *Nature* **467:**211–213.

Trausch B, Oertel R, Richter K, and Gramatté T (1995) Disposition and bioavailability of the β_1-adrenoceptor antagonist talinolol in man. *Biopharm Drug Dispos* **16:**403–414.

Urnov FD, Rebar EJ, Holmes MC, Zhang HS, and Gregory PD (2010) Genome editing with engineered zinc finger nucleases. *Nat Rev Genet* **11:**636–646.

Zhou SF (2008) Structure, function and regulation of P-glycoprotein and its clinical relevance in drug disposition. *Xenobiotica* **38:**802–832.

Address correspondence to: Dr. Myung Kyun Shin, Merck Sharp and Dohme Corp., RY80Y-310, 126 East Lincoln Ave., Rahway, NJ 07065. E-mail: myung.shin2@merck.com